Vaccine 34 (2016) 1259–1267

Contents lists available at ScienceDirect

Vaccine

journal homepage: www.elsevier.com/locate/vaccine

High-throughput characterization of virus-like particles by interlaced size-exclusion chromatography

Christopher Ladd Effio[a], Stefan A. Oelmeier[a,b], Jürgen Hubbuch[a,*]

[a] Karlsruhe Institute of Technology, Institute of Process Engineering in Life Sciences, Section IV: Biomolecular Separation Engineering, Karlsruhe, Germany
[b] Boehringer Ingelheim Pharma GmbH & Co. KG, Germany

ARTICLE INFO

Article history:
Received 15 October 2015
Received in revised form 12 January 2016
Accepted 17 January 2016
Available online 1 February 2016

Keywords:
Virus-like particle vaccines
Size-exclusion HPLC
Papillomavirus
Aggregates
High-throughput analytics
Process analytical technology

ABSTRACT

The development and manufacturing of safe and effective vaccines relies essentially on the availability of robust and precise analytical techniques. Virus-like particles (VLPs) have emerged as an important and valuable class of vaccines for the containment of infectious diseases. VLPs are produced by recombinant protein expression followed by purification procedures to minimize the levels of process- and product-related impurities. The control of these impurities is necessary during process development and manufacturing. Especially monitoring of the VLP size distribution is important for the characterization of the final vaccine product. Currently used methods require long analysis times and tailor-made assays. In this work, we present a size-exclusion ultra-high performance liquid chromatography (SE-UHPLC) method to characterize VLPs and quantify aggregates within 3.1 min per sample applying interlaced injections. Four analytical SEC columns were evaluated for the analysis of human B19 parvo-VLPs and murine polyoma-VLPs. The optimized method was successfully used for the characterization of five recombinant protein-based VLPs including human papillomavirus (HPV) VLPs, human enterovirus 71 (EV71) VLPs, and chimeric hepatitis B core antigen (HBcAg) VLPs pointing out the generic applicability of the assay. Measurements were supported by transmission electron microscopy and dynamic light scattering. It was demonstrated that the iSE-UHPLC method provides a rapid, precise and robust tool for the characterization of VLPs. Two case studies on purification tools for VLP aggregates and storage conditions of HPV VLPs highlight the relevance of the analytical method for high-throughput process development and process monitoring of virus-like particles.

1. Introduction

In recent years, promising prophylactic and therapeutic vaccination prospects for public health threats have arisen from the development of virus-like particles (VLPs). VLPs are protein assemblages which are produced by recombinant expression of viral structural proteins [1,2]. Thus, the structure of highly pathogenic viruses such as HIV [3], Influenza [4] and Ebola [5] can be mimicked or tailor-made nanocarriers for antigenic epitope presentation [6–9] can be designed. Due to production in genetically modified organisms, the analysis of product-related and process-related impurities is important during development and manufacturing of VLP vaccines [10,11]. Process-related impurities such as host cell proteins (HCPs) and DNA can be rapidly assessed by methods standardized in the biopharmaceutical industry for therapeutic proteins [12]. In contrast, quantitative analysis of product-related impurities such as aggregates is more challenging and mostly tailor-made for each vaccine due to the large size and complexity of VLPs. Traditionally, VLP characterization is often done by transmission electron microscopy (TEM) requiring high investment costs, extensive sample and instrument preparation work, and specialized staff. A rapid technology for VLP characterization is dynamic light scattering (DLS) [13–15]. The method allows the determination of hydrodynamic particle diameters by measuring the fluctuations of light scattering from particles in solution. However, DLS is less sensitive in resolving aggregates [16]. Currently used quantitative methods for VLP aggregates are asymmetrical flow field-flow fractionation (AF4) [17,18,16], disc centrifugation particle size analysis [19], electrospray differential mobility analysis [18], and size-exclusion chromatography (SEC) [20]. These techniques are very time-consuming with analysis times ranging from 30 to 60 min per sample [17,18,16,20]. SEC is the most widely used technique for aggregate quantification in the biopharmaceutical

* Corresponding author. Tel.: +49 072160842557.
E-mail address: juergen.hubbuch@kit.edu (J. Hubbuch).
URL: http://mab.blt.kit.edu (J. Hubbuch).

http://dx.doi.org/10.1016/j.vaccine.2016.01.035
0264-410X/

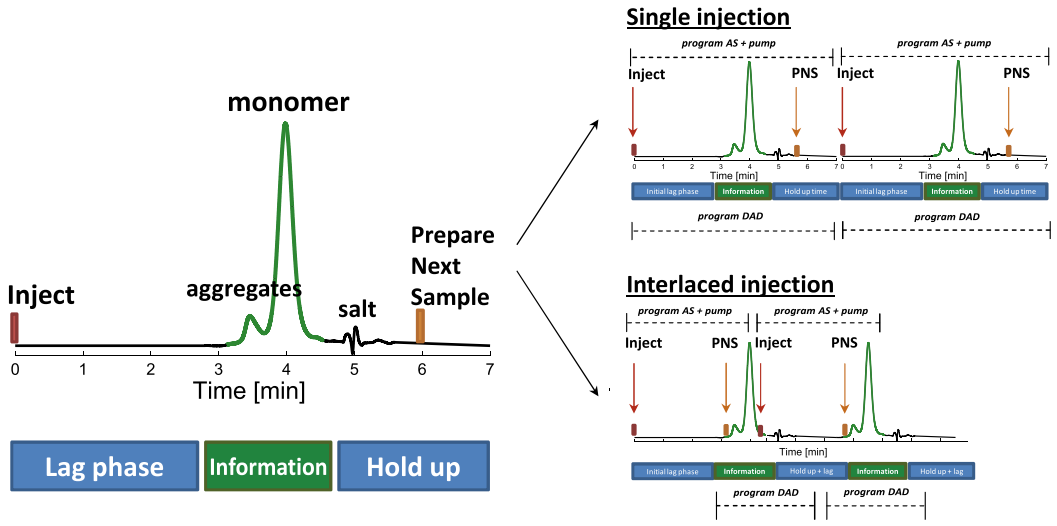

Fig. 1. Schematic illustration of SEC chromatograms for single- and interlaced-injection mode of an analyte containing aggregates and monomer. Information phases are marked by green colored bars, lag and hold-up phases by blue colored bars. Timelines for the program of the autosampler (AS) and pump and the diode array detector (DAD) are presented for two sequent injections in single- and interlaced-injection mode. (For interpretation of references to color in this figure legend, the reader is referred to the web version of the article.)

industry [21]. SEC methods have been successfully applied for process monitoring of capsomere vaccines [22], recombinant fusion protein vaccines [15], and human hepatitis B virus surface antigen (HBsAg) VLPs [23–26]. Recently, rapid size-exclusion ultra-high performance liquid chromatography (SE-UHPLC) methods have been realized for monoclonal antibodies by performing interlaced sample injections with analysis times of 2–6 min [27,28]. Fig. 1 shows a schematic drawing of the principle of interlaced SEC (iSEC) methods. The 'information phase' (*green*) in a SEC run is the time range including the elution of relevant species (aggregates, monomer). The longest phase in a classical single injection SEC method run is the 'lag phase' (*blue*), which is the time range from injection to elution of the first species. The 'hold- up' (*blue*) phase refers to the time from the end of the information phase to the column's void time defined by the elution of small molecules such as salts. In order to reduce the total analysis time of SEC methods without changing the performance of 'information phases', the 'lag phase' can be eliminated by injecting subsequent samples prior to the complete elution of previous sample components. This operation is referred to as interlaced injection mode.

In this work, we present the development and application of an iSE-UHPLC method for recombinant protein-based VLPs. The feasibility of the assay was evaluated for human papilloma (HPV) VLPs [29], human enterovirus 71 (EV71) VLPs [30], murine polyomavirus (MuPyV) VLPs [7], human B19 parvo (B19 VP1/VP2) VLPs [31]., and chimeric hepatitis B core antigen (HBcAg) VLPs [8]. Two case studies are presented for the application of the iSE-UHPLC during downstream process development and stability studies. The designed method allows a rapid assessment of VLP dispersity and is well-suited for high-throughput pharmaceutical process development of VLPs.

2. Materials and methods

2.1. Disposables

For precipitation screenings, sample storage, fractionation by FPLC and UHPLC, 350 μL-polypropylene plates (Greiner Bio-One, Kremsmünster, Austria) were used. Stability studies with HPV VLPs were performed in 1.5 mL-polypropylene Eppendorf® Safe-Lock Tubes (Eppendorf, Hamburg, Germany). Frozen VLPs were thawed and centrifuged in the same tubes at 18,000 × *g* and 4 °C for 10 min.

2.2. Chemicals and buffers

For the SE-UHPLC method, K_2HPO_4 was obtained from VWR BDH Prolabo (Radnor, Pennsylvania, USA). MOPS was purchased from Carl Roth GmbH & Co. KG (Karlsruhe, Germany). The SEC standard proteins thyroglobulin from bovine thyroid and uracil were purchased from Sigma–Aldrich (St. Louis, MO, USA) and Alfa Aesor (Ward Hill, MA, USA), respectively. All other chemicals were obtained from Merck KGaA (Darmstadt, Germany). All buffer solutions were prepared with ultra pure water drawn from a water purification system provided by Sartorius (Goettingen, Germany). UHPLC analysis was conducted with buffers composed of 0.2 M K_2HPO_4 and 0.25 M KCl. The pH value was set at pH 7.0 for characterization studies with HPV VLPs and pH 7.4 for the SEC analysis of other VLPs. Semi-preparative purifications of B19 VP1/VP2 VLPs were performed by aqueous two-phase extraction and precipitation with PEG 4000 as described previously [32] and by anion-exchange membrane chromatography [33]. PBS buffer at pH 7.4 was used as mobile-phase buffer for chromatography experiments with a semi-preparative SEC column.

2.3. Virus-like particles

The general applicability of an interlaced SE-UHPLC method for VLP characterization was evaluated with several purified VLPs differing in size, morphology, expression hosts, and number of viral proteins. An overview of analyzed VLPs is given in Table 1.

Purified HPV VLPs (HPV type 33 [29]) derived from yeast cells were kindly provided by Merck & Co (Kenilworth, NJ, USA) at a concentration of 0.8 mg/mL in a buffer containing histidine and polysorbate 80 (pH 6.2). MuPyV VLPs were produced at shaker flask scale in *Escherichia coli* cells, purified as published by Middelberg et al. [7], and dialyzed into PBS (pH 7.4) yielding a concentration of 0.3 mg/mL. EV71 VLPs derived from *Spodoptera frugiperda Sf*9 insect cells were kindly supplied by Sentinext Therapeutics (Penang, Malaysia) in a Tris buffer (pH 7.5) at a concentration of 0.1 mg/mL. Chimeric HBcAg VLPs with fused tumor epitopes were expressed in *E. coli* and generously provided by BioNTech Protein

Table 1
Overview of evaluated virus-like particles. BEVS/IC: baculovirus expression vector/ insect cell system; EV: enterovirus; HBcAg: hepatitis B core antigen; HBV: hepatitis B virus; HPV: human papilloma virus; MuPyV: murine polyomavirus.

Virus	Family	Expression system	Recombinant protein	Diameter	References
HPV	Papillomaviridae	*S. cerevisiae*	L1 (55 kDa)	40–60 nm	[39,14]
MuPyV	Polyomaviridae	*Escherichia coli*	VP1 (42 kDa)	40–50 nm	[7]
HBV	Hepadnaviridae	*Escherichia coli*	core antigen (21 kDa)	30–34 nm	[48]
EV 71	Picornaviridae	BEVS/IC	VP1 (33 kDa), VP2 (28 kDa), VP3 (27 kDa), VP4 (8 kDa)	25–35 nm	[41,49]
Parvovirus B19	Parvoviridae	BEVS/IC	VP1 (83 kDa), VP2 (58 kDa)	25–30 nm	[50,31,32]

Therapeutics (Mainz, Germany) in a Tris buffer (pH 7.2) at a concentration of 2.18 mg/mL. B19 VP1/VP2 VLPs derived from *Sf*9 insect cells were kindly provided by Diarect AG (Freiburg, Germany) at a concentration of 0.5 mg/mL in a phosphate buffer (pH 7.4). In general, VLPs were stored at −80 °C and centrifuged (18,000 × *g*, 4 °C, 10 min) prior to analysis by SE-UHPLC, DLS or TEM.

2.4. Size-exclusion ultra-high performance liquid chromatography

SE-UHPLC analysis was performed on an UltiMate® 3000 RSLC × 2 Dual system provided by Thermo Fisher Scientific (Waltham, MA, USA). The UHPLC consisted of a HPG-3400RS pump module, a WPS-3000 autosampler, a TCC-3200 column oven, and a DAD3000 detector. System control and peak integration was done with the software Chromeleon® 6.80 (Thermo Fisher Scientific, Waltham, MA, USA). Sample injection was done by full-loop injection with a 20 μL sample loop, a 15 μL injection needle, and a 250 μL syringe. Samples were cooled in the autosampler at 8 °C prior to column experiments which were performed at 25 °C. UHPLC measurements were conducted in triplicates. The feasibility of a VLP aggregate separation by SEC was evaluated with B19 VP1/VP2 VLPs and MuPyV VLPs comparing four different columns: TSKGel G5000 PWxl [16] (Tosoh Bioscience, Stuttgart, Germany), TSKGel G6000 PWxl (Tosoh Bioscience, Stuttgart, Germany), ACQUITY UPLC Protein BEH450 (Waters Corporation, Milford, MA, USA), and SRT SEC-1000 (Sepax Technologies, Newark, DE, USA). An overview of column characteristics and applied flow rates is given in Table 2.

Interlaced SEC (iSEC) experiments were realized using the SRT SEC-1000 column at a flow rate of 0.8 mL/min by shifting the 'PrepareNextSample' ('PNS') and the 'Inject' commands of subsequent samples to earlier points in time (Fig. 1). As explained in detail by Diederich et al. [28], the system was split into two virtual parts in order to record the information phase of each sample separately. In timebase I, settings for pump, autosampler, and column compartment were controlled, while timebase II controlled the DAD (Fig. 1).

2.5. Dynamic light scattering

For comparison of iSE-UHPLC results, VLP samples were analyzed by dynamic light scattering (DLS) to determine the hydrodynamic diameter and the polydispersity index (PdI) of VLPs. DLS measurements were performed using a Malvern Zetasizer Nano ZSP (Malvern Instruments, Worcestershire, UK). The DLS-based aggregate content was determined by the volume distribution which assumes the presence of spherical particles. Measurements were performed in triplicates.

2.6. Transmission electron microscopy

Transmission electron microscopy (TEM) micrographs were taken on a Philips CM 200 FEG/ST transmission electron microscope at 200 kV from all VLP samples to visualize the VLP size, dispersity, and morphology. The sample preparation procedure has been described earlier [32].

2.7. Purification methods for aggregate removal

SEC and precipitation with polyethylene glycol (PEG) were evaluated as potential unit operations for the separation of B19 VP1/VP2 VLPs and VLP aggregates. An ÄKTA-purifier 10 fast protein liquid chromatography (FPLC) (GE Healthcare, Uppsala, Sweden) was used for semi-preparative purifications of B19 VP1/VP2-VLPs. B19 VP1/VP2 VLPs were isolated from *Sf*9 insect cells by sonication and subsequent solid–liquid separation steps as described previously [32]. Initial purification was performed by anion-exchange (AEX) membrane chromatography using 3 mL Sartobind® Q membrane (Sartorius AG, Goettingen, Germany). The method has recently been described by our group [33]. The majority of HCPs, baculoviruses, and DNA were separated by a bind-and-elute process with three salt steps (0.3 M NaCl (step I), 0.38 M NaCl (step II), and 1 M NaCl (step III)). Pre-purified VLPs (pooled fractions from AEX membrane step II) were finally injected on a Superose® 6 Increase 10/300 column (GE Healthcare, Uppsala, Sweden) at a flow rate of 38 cm/h (0.5 mL/min) to investigate the separation of VLP aggregates. Precipitation studies with polyethylene glycol (PEG) 4000 were conducted on a robotic liquid handling station. A Tecan Freedom EVO® 200 system (Tecan, Crailsheim, Germany) was used as liquid handling platform (Tecan, Crailsheim, Germany). Liquid handling calibration, set-up, and the precipitation screening method were described earlier [34,35]. In brief, 300 μL systems with different PEG concentrations and constant VLP concentrations were prepared in 96-well plates in triplicates by mixing ultra pure water, a 40% [w/w] PEG 4000 stock solution, and pre-purified B19 VP1/VP2-VLPs. Systems were mixed on an orbital shaker, centrifuged, and supernatant samples were diluted four fold with PBS prior to analysis by iSE-UHPLC.

Table 2
Applied analytical size-exclusion chromatography columns for large biomolecules.

Column	Dimension (mm)	Particle size (μm)	Pore size (Å)	Max. pressure (bar)	Flow rate (cm/h)
TSKGel G5000 PWxl	7.8 × 300	10	1000	20	100 (0.8 mL/min)
TSKGel G6000 PWxl	7.8 × 300	13	>1000	20	100 (0.8 mL/min)
ACQUITY UPLC BEH450	4.6 × 150	2.5	450	310	144 (0.4 mL/min)
SRT SEC-1000	4.6 × 300	5	1000	241	217–361 (0.6–1 mL/min)

2.8. Stability studies with HPV VLPs

The dispersity of HPV VLPs was assessed under several stress conditions to identify critical parameters which might trigger the formation of VLP aggregates. Chemical stress was applied by exchanging the buffer from the formulation buffer containing stabilizing agents to phosphate and MOPS buffers with varying ionic strengths. Subsequently, buffer-exchanged VLPs were stored for 3 d at 8 °C prior to analysis. Thermal stress was applied by incubating VLP samples on an orbital shaker at 300 rpm for 1–5 h at 40 °C. Incubation at 1400 rpm, 15 °C in 1.5 mL-polypropylene Eppendorf® Safe-Lock Tubes with a sample volume of 300 μL was performed to trigger mechanical stress on VLPs. Freeze-thaw stress was applied by freezing the samples in 1.5 mL-polypropylene Eppendorf® Safe-Lock Tubes in liquid nitrogen and thawing them at 25 °C.

3. Results and discussion

3.1. Development of an interlaced SEC-UHPLC method

In the International Conference on Harmonization (ICH) guideline Q2 [36] on the validation of analytical procedures, it is suggested to verify among others the specificity, precision, linearity, and robustness of novel methods for biopharmaceutical products. The initial objective was therefore to identify an analytical column separating VLPs and VLP aggregates in order to develop a specific analytical method. A pre-selection of columns was done based on pore sizes (>300 Å) and published SEC studies with VLPs [23–26]. Subsequently, column performances were compared by applying B19 VP1/VP2 VLP and MuPyV VLP samples. Fig. 2a shows an overlay of UV chromatograms derived from the analysis of 8 μg B19 VP1/VP2 VLPs, while Fig. 2b displays the overlay of UV chromatograms for SEC runs with 3 μg MuPyV VLPs. In each chromatogram, the UV absorption at 226 nm is plotted against the mobile-phase volume. Due to different column void volumes, the elution volumes of VLP components differ between the columns. The void volumes are 2.1 mL for the Acquity BEH 450 column (black solid line), 3.9 mL for the SRT 1000 column (blue solid line), 12.1 mL for the TSKgel G5000 PWxl column (black dotted line), and 12.3 mL for the TSKgel G6000 PWxl column (red dotted line). This implies a lower buffer consumption for SEC runs with Acquity and SRT columns than with TSKgel columns. Neglecting the UV peaks close to the void volumes, only the SRT 1000 column shows multiple peaks for the VLP samples: The elution of B19 VP1/VP2 VLPs is split into three peak groups with two minor and one major peak, while the elution of MuPyV VLPs reveals one minor and one major peak. Peak fractionation and analysis by SDS-PAGE evidenced the presence of major viral proteins in all three UV peaks of the B19 VP1/VP2 VLP sample and in the two UV peaks of MuPyV VLPs (data not shown). Moreover, the total peak areas in the SEC chromatograms generated with the SRT 1000 column are higher than in those generated with other columns. This suggests a higher recovery and less secondary interactions of VLP components with the SRT 1000 column matrix. The weaker performance of other evaluated columns was attributed to different base materials (methacrylate vs. silica) and pore sizes (450 Åvs. 1000 Å). It must be noted that both peak resolution and recovery might have been higher for all columns at lower flow rates. However, the main goal of this work was to develop a rapid analytical procedure for VLP aggregates.

In Fig. 2c, the elution of MuPyV VLPs is compared with the elution of a protein standard composed of thyroglobulin and uracil. The UV chromatogram of the MuPyV VLPs demonstrates that the major peak at 3.09 mL elutes prior to thyroglobulin (3.38 mL, 17 d nm [37]) and thyroglobulin aggregates (3.22 mL) indicating a larger

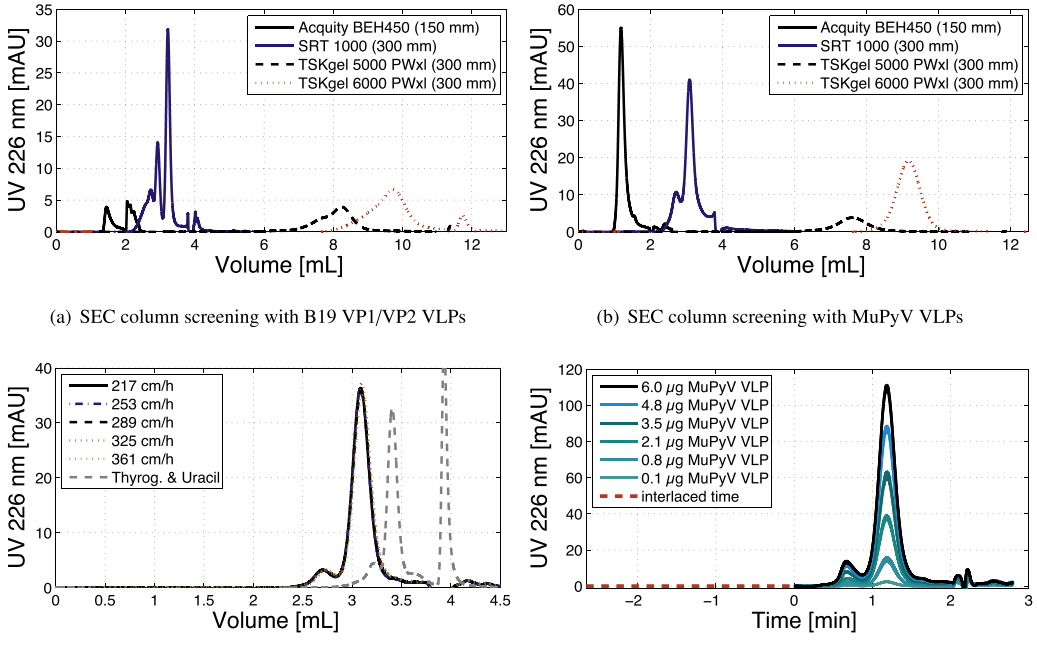

(a) SEC column screening with B19 VP1/VP2 VLPs

(b) SEC column screening with MuPyV VLPs

(c) Flow rate effect for SRT 1000 column

(d) Interlaced SEC mode for MuPyV VLPs

Fig. 2. Development steps of an interlaced SE-UHPLC method for VLPs. Chromatograms represent the mean of triplicate determinations. (a) Overlaid chromatograms of 8 μg human B19 parvo (B19 VP1/VP2) VLPs injected on an Acquity BEH450 (black solid line), SRT 1000 (blue solid line), TSKgel G5000 PWxl (black dotted line), and TSKgel G6000 PWxl column (red dotted line). (b) Overlaid chromatograms of 3 μg murine polyomavirus (MuPyV) VLPs injected on an Acquity BEH450 (black solid line), SRT 1000 (blue solid line), TSKgel G5000 PWxl (black dotted line) and TSKgel G6000 PWxl column (red dotted line). (c) Overlay of chromatograms of 2.1 μg MuPyV VLPs for an SRT 1000 column at varying flow rates. The elution profile of a protein standard composed of thyroglobulin and uracil is plotted as gray dotted line. (d) Chromatogram of MuPyV VLPs injected on an SRT 1000 column in interlaced-injection mode at a flow rate of 0.8 mL/min. Increasing VLP masses were loaded on the column and are plotted in triplicates. Samples were injected at −2.66 min (DAD timebase) as indicated by the red dotted line illustrating the interlaced injection time. (For interpretation of references to color in this figure legend, the reader is referred to the web version of the article.)

size for the MuPyV VLPs and B19 VP1/VP2 VLPs. Due to the highest selectivity and recovery, the SRT 1000 column was selected for all subsequent experiments. In the following, the impact of the mobile-phase flow was evaluated to test the robustness and to accelerate the method. Fig 2c shows the overlay of chromatograms generated with 2.1 μg MuPyV VLPs at flow rates ranging from 217 to 361 cm/h (0.6–1 mL/min). Chromatograms were hardly influenced by the flow rate in the examined range. This allows a high-throughput of samples even in single-injection mode and demonstrates that high back pressure of up to 240 bar at 1 mL/min did not increase VLP aggregate levels. Similar observations were recently made for monoclonal antibodies analyzed by SE-UHPLC at high back pressure [38].. For the implementation of an iSEC method, an operating flow rate of 289 cm/h (0.8 mL/min) was chosen. The analysis time at this flow rate was 6.0 min with an initial lag phase of 3.1 min for MuPyV VLP aggregates and 2.7 min for B19 VP1/VP2 VLP aggregates. In the iSEC method, the start of timebase II (DAD) was triggered at 2.66 min of timebase I (autosampler and pump) to ensure the detection of the largest molecules eluting in the exclusion volume of the column. At 0.34 min of timebase II, the injection of the next sample in timebase I was triggered. The 'PrepareNextSample' was set at 1.7 min of timebase I to ensure a total analysis time of 3.1 min per sample. Fig. 2d shows the chromatogram of overlaid triplicate injections of varying MuPyV VLP concentrations. The UV signal is plotted against the DAD aquisition time (timebase II). Thus, the red dotted line illustrating the interlaced time shows that the sample injection was performed at −2.66 min which corresponds to 0 min of timebase I. The elution profile with two major peaks steadily increasing for higher loadings does not differ at all from the chromatograms generated by the single-injection mode. This underlines both repeatability and linearity of the iSEC method for the analysis of MuPyV VLPs. Furthermore, it is shown that the presence and ratio of the two major peaks do not depend on the injected VLP mass in the investigated range.

3.2. Characterization of virus-like particles by iSE-UHPLC, TEM and DLS

The developed iSEC method was evaluated for several VLPs in order to test the general applicability of the method. Moreover, an important issue was whether different peaks in iSEC chromatograms were created by VLPs of varying sizes or by VLPs of the same size forming VLP aggregates. Therefore, samples were analyzed by iSE-UHPLC, TEM, and DLS. Fig. 3 shows an overview of

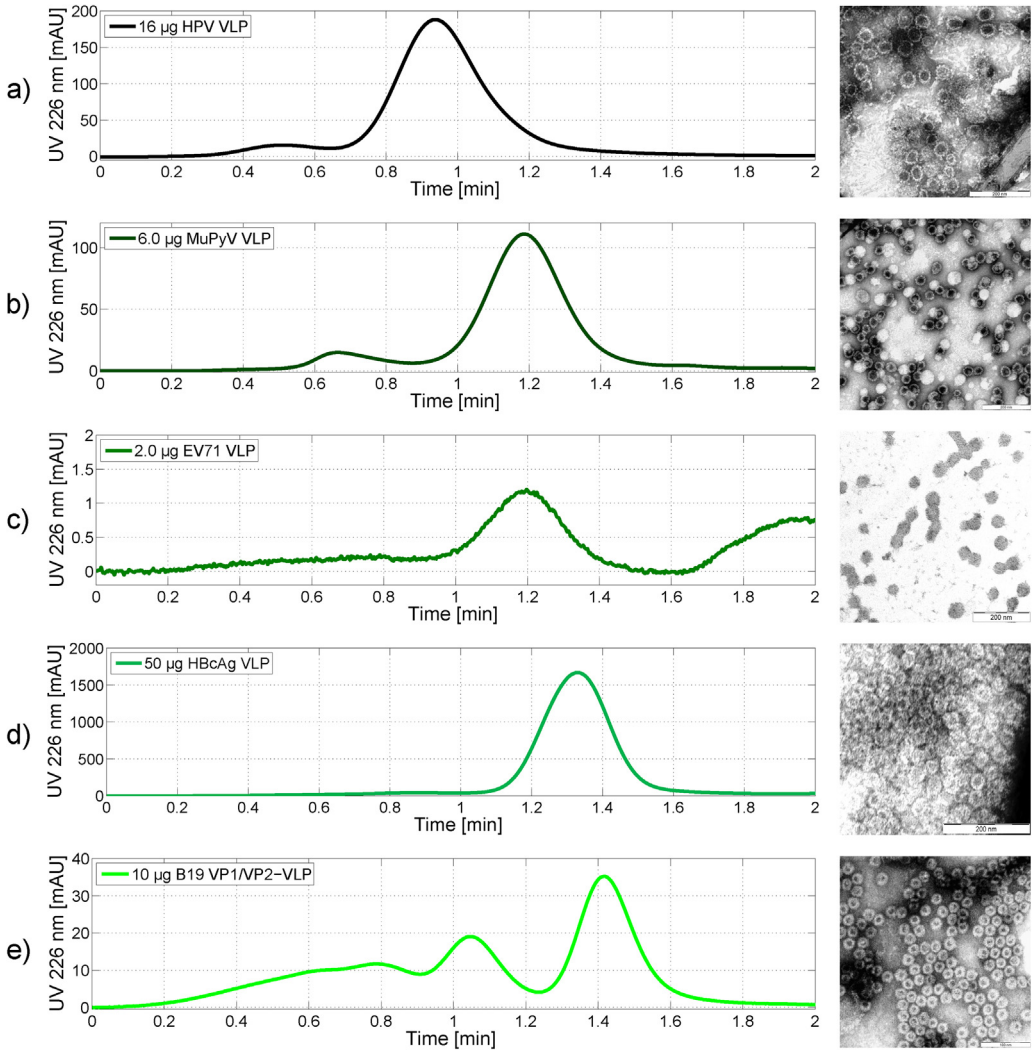

Fig. 3. Characterization of virus-like particles by interlaced SE-UHPLC and transmission electron microscopy (TEM). Chromatograms and TEM micrographs are arranged according to decreasing particle sizes: (a) 16 μg human papilloma (HPV) VLPs, (b) 6.0 μg murine polyomavirus (MuPyV) VLPs, (c) 2.0 μg human enterovirus 71 (EV71) VLPs, (d) 50 μg chimeric HBcAg VLPs, and (e) 10 μg human B19 parvo (B19 VP1/VP2) VLPs.

Table 3
Summary of VLP characterization by dynamic light scattering (DLS) and interlaced SEC (iSEC) UHPLC. Retention times according to iSE-UHPLC are given for the elution of VLP monomers.

VLP/Protein	Average size [d.nm]	PdI (DLS)	Aggregates (DLS) [% v/v]	Aggregates (iSEC) [%]	Retention time (iSEC) [min]
HPV VLP	60.8	0.134	0	5.8 ± 0.2	0.93
MuPyV VLP	65.1	0.216	0	8.2 ± 0.4	1.19
EV 71	55.9	0.204	0	14 ± 3.0	1.2
HBcAg VLP	40.3	0123	0	1.4 ± 0.2	1.33
B19 VP1/VP2 VLP	211.1	0.467	51.5	55.8 ± 0.5	1.42

iSE-UHPLC and TEM measurements for five different VLPs, while Table 3 lists the results obtained from DLS measurements.

The UV chromatograms in Fig. 3 are plotted against the measurement time of timebase II. In the following, only UV peaks with retention times below the iSEC retention time of thyroglobulin (1.56 min) are discussed. The chromatogram in Fig. 3a reveals two UV peaks for a sample containing 16 μg HPV VLPs, while the TEM micrograph displays spherical particles with pentamer structures and a total particle size of 45–60 nm. Similar particle diameters and structures were observed by Zhao et al. [39,14] for HPV VLPs derived from yeast cells. In the TEM micrographs, there were not any VLPs detected with a size larger than 65 nm, while DLS analysis determined a mean particle size of 60.8 d nm for HPV VLPs (Table 3). Hence, the first peak in the iSEC chromatogram (0.52 min) is probably attributed to the formation of VLP aggregates as reported by Deschuyteneer et al. [19]. The aggregate level in the HPV VLP sample was 5.8 ± 0.2% according to the iSEC method, while no aggregates were detected by DLS measurements (Table 3). For MuPyV VLPs, the iSEC chromatogram in Fig. 3b looks similar as for HPV VLPs with one minor (0.68 min) and one major UV peak (1.19 min). Again, TEM micrographs display spherical particles with a similar morphology as HPV VLPs and particle sizes of 40–50 nm. The VLP aggregate level was 8.2±0.4% according to iSE-UHPLC. The presence of aggregates in MuPyV VLP preparations has also been reported by Pease et al. [18] and Mohr et al. [40]. Fig. 3c shows the iSEC chromatogram of 2.0 μg EV71 VLPs. The major peak elutes at 1.2 min. The UV absorption signal is noisy and low with a maximum at 1.2 mAU demonstrating that observed peaks are close to the detection limit of the DAD. This impedes the exact quantification of VLP aggregates. Despite a low concentration, the presence of spherical particles in the EV71 VLP sample is demonstrated by the TEM micrograph. In contrast to other analyzed VLPs revealing empty particles, EV71 VLPs appeared as solid particles with diameters of 35–50 nm as observed by Liu et al. [41]. According to DLS measurements, the average particle size for EV71 VLPs was 55.9 nm and no aggregates were detected. In Fig. 3d, the iSEC chromatogram and TEM micrograph of 50 μg chimeric HBcAg VLPs are displayed. The chromatogram shows a uniform dispersity with one major peak eluting at 1.33 min. The TEM micrograph illustrates a high number of empty particles with diameters ranging from 35 to 40 nm. The mean particle diameter determined by DLS was 40.3 nm. The aggregate level according to the iSE-UHPLC method was 1.4 ± 0.2%, while no aggregates were detected by DLS measurements. Fig. 3e displays the chromatogram of a sample containing 10 μg B19 VP1/VP2 VLPs. Three UV peaks eluting at 0.6 min, 1.04 min, and 1.42 min indicate a polydisperse distribution. In contrast, the TEM micrograph shows homogeneous icosahedral empty particles with a size of 25–30 nm. Considering the elution times of thyroglobulin (1.56 min, 17 d nm [37]) and HPV VLPs (0.93 min, 60 d nm), the UV peak at 1.42 min shows probably the elution of B19 VP1/VP2 VLPs while the other two peaks are attributed to aggregates of two (1.04 min) and more VLPs (0.6 min). Both DLS and iSE-UHPLC analysis evidence an aggregate level above 50% (Table 3). Such an unusually high amount of aggregates in B19 VP1/VP2 VLP samples has not yet been reported elsewhere. Since B19 VP1/VP2 VLPs are evaluated as human vaccine candidates against diseases attributed to parvovirus infections [31], the impact of aggregates on safety, immunogenicity and reactogenicity of a VLP vaccine should be carefully evaluated in the future. Skin reactions reported in a clinical phase study with a B19

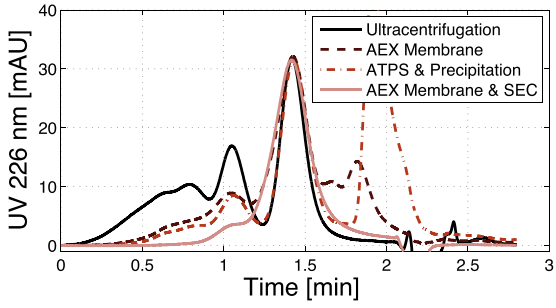

(a) UHPLC chromatograms for VLPs purified by different downstream processes

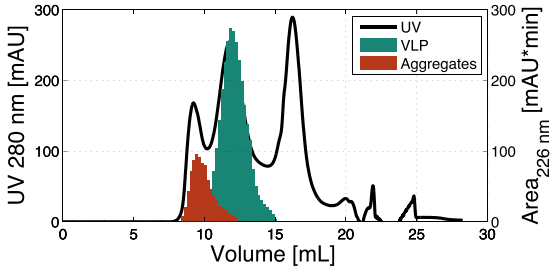

(b) Separation of VLP aggregates by SEC

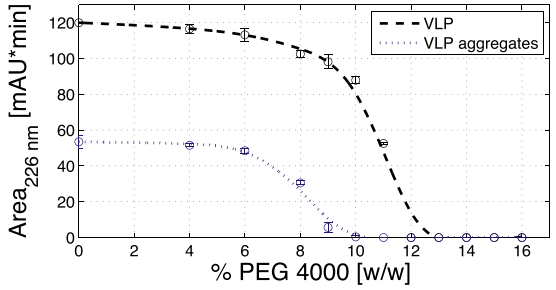

(c) Separation of VLP aggregates by SEC

Fig. 4. Comparison of purification tools for the separation of VLP aggregates from human B19 parvo (B19 VP1/VP2) VLPs. (a) UHPLC chromatograms for VLPs purified by ultracentrifugation (black solid line), anion-exchange (AEX) membrane chromatography (purple dotted line), aqueous two-phase extraction (ATPS) and precipitation (red dotted line), and AEX membrane chromatography and SEC (rose solid line). (b) Chromatogram of a B19 VP1/VP2 VLP polishing step on a Superose® 6 Increase column tracking VLPs (green bars) and VLP aggregates (red bars). (c) Solubility curves for 0.5 mg/mL B19 VP1/VP2 VLPs tracking VLPs (black) and VLP aggregates (blue) at increasing concentrations of polyethylene glycol 4000. (For interpretation of references to color in this figure legend, the reader is referred to the web version of the article.)

VP1/VP2 VLP vaccine candidate [42] might have been attributed to increased levels of VLP aggregates.

Summarizing the VLP characterization by the developed iSE-UHPLC method, it could be demonstrated that a resolution of VLPs and VLP aggregates in the size range of 20–120 nm is feasible. Although the DLS results listed in Table 3 indicated the presence of aggregates in the B19 VP1/VP2 VLP sample, no aggregates were detected by the method for other VLP samples. Nevertheless, the polydispersity index (PdI) given by the DLS instrument correlates with the aggregate level determined by the iSEC method. The lowest PdI of 0.123 was determined for HBcAg VLPs containing 1.4% aggregates, while the highest PdI of 0.467 was identified for B19 VP1/VP2 VLPs containing 55.8% aggregates. Comparing results from DLS, TEM and iSE-UHPLC analysis, the iSEC method provides a precise high-throughput analytical technique for VLPs.

3.3. Purification tools for the separation of VLP aggregates

In the following, the developed iSE-UHPLC method was applied for the assessment of VLP purification procedures. The characterization of VLPs has revealed the presence of aggregates in all measured VLP samples. The propensity of aggregate formation during VLP processing can be manipulated by adding stabilizers such as detergents, sugars or polyols into process buffers [40,43]. However, irreversible aggregates also form during expression in cell culture, and apart from stabilization procedures, there is a demand for separation techniques for VLP aggregates. In this work, the highest aggregate level was determined for B19 VP1/VP2 VLPs making these particles attractive to evaluate the effect of downstream processing on the aggregate level. Fig. 4a shows the iSEC chromatogram of the same VLP insect cell feedstock purified by different purification procedures. Chromatograms are normalized to the VLP monomer peak at 1.42 min to highlight varying aggregate levels. The residual DNA levels were below 20 ng/mL, and protein purities varied between 81% (AEX membrane sample [33]) and 99% (ultracentrifugation sample) according to measurements by picogreen assay and capillary gel electrophoresis (data not shown). The elution profiles demonstrate that peaks eluting between 0 and 1.2 min show the highest UV areas for VLPs purified by ultracentrifugation (55.8 ± 0.5%) and the lowest for VLPs purified by a combination of AEX membrane chromatography and SEC [33] (5.9 ± 0.4%). Moreover, VLP samples purified by an ATPS and precipitation procedure revealed a lower aggregate level (27.5 ± 0.4%) than VLPs purified by AEX membrane chromatography (30.7 ± 0.7%). These findings suggest that a separation of aggregates might be feasible by both chromatographic and non-chromatographic unit operations.

Fig. 4b shows the chromatogram of a VLP aggregate separation by size-exclusion chromatography on an FPLC system. 1500 μg B19 VP1/VP2 VLPs purified by AEX membrane chromatography were injected on a Superose® 6 Increase 10/300 column. VLP monomers (*green bars*) and VLP aggregates (*red bars*) were tracked by the iSE-UHPLC method. The elution profile displays three major peaks for the VLP sample: VLP aggregates (9.1 mL), VLP monomers (11.5 mL), and residual HCPs (16.4 mL). Hence, a separation of VLP aggregates was also rendered with a preparative SEC resin. In Fig. 4c, iSEC UV peak areas of VLP monomers (*black dotted line*) and VLP aggregates (*blue spotted line*) are plotted against increasing concentrations of PEG 4000. Data points are interpolated with lines to guide the eye and represent the soluble fraction of each component at a certain PEG concentration. A decrease of solubility is observed at different PEG concentrations for VLP monomers and VLP aggregates. While VLP aggregates precipitated thoroughly at 10% [w/w] PEG 4000, about 81 ± 2% VLP monomers were detected in the soluble fraction at this concentration. Thus, a separation of irreversible VLP aggregates might be realized by adding PEG to a VLP sample, performing a solid–liquid separation and finally formulating VLPs in a stabilizing buffer to prevent the formation of new aggregates. A similar approach has, for instance, been used for the separation of IgG aggregates by Giese et al. [44].

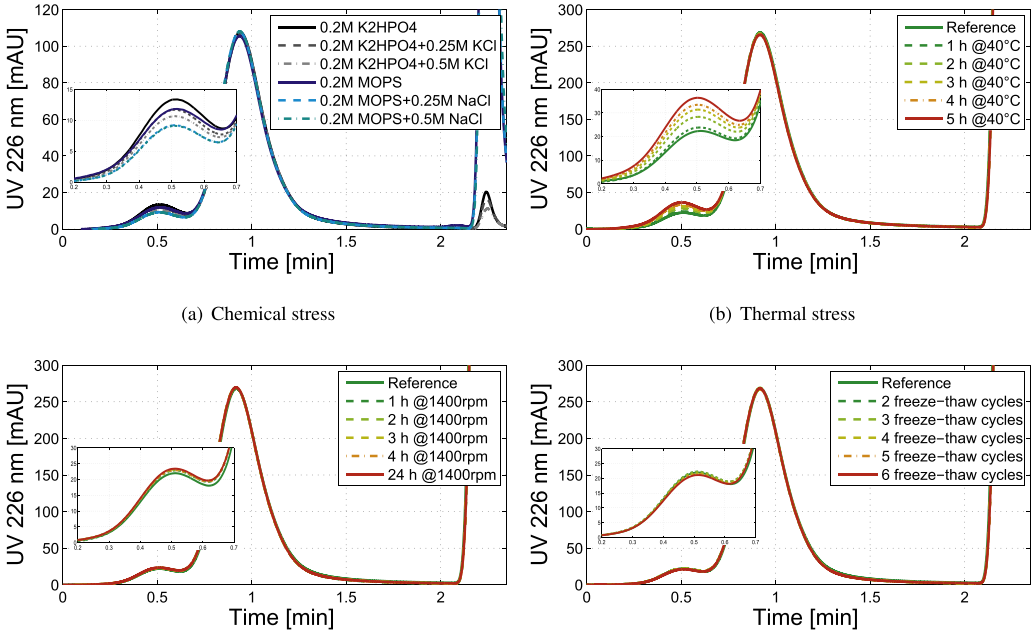

(a) Chemical stress

(b) Thermal stress

(c) Mechanical stress

(d) Freeze-thawing

Fig. 5. Characterization of human papilloma (HPV) VLPs under different stress conditions. (a) The impact of ionic strength on the formation of aggregates was assessed by storing 0.4 mg/mL VLPs in different buffer solutions for 3 d at 8 °C. (b) Thermal stress was applied by heating 0.8 mg/mL VLPs at 40 °C for 1–5 h. (c) Mechanical stress was applied by incubating 0.8 mg/mL VLPs on an orbital shaker at 1400 rpm for 1–24 h. (d) Stress by freeze-thawing was applied by 2–6 cycles of freezing in liquid nitrogen with subsequent thawing at room temperature at a VLP concentration of 0.8 mg/mL. VLPs underwent the first freeze-thaw cycle upon sample preparation.

3.4. Effect of process conditions on the stability of HPV VLPs

The propensity to form aggregates varies for each VLP depending on structural characteristics and process conditions such as pH, ionic strength, temperature, shear forces, freeze–thaw cycles or interactions with equipment surfaces. The developed iSE-UHPLC method is a rapid assay to evaluate the effect of such process conditions on VLPs. In a case study, HPV VLPs with a comparably low level of aggregates ($5.8 \pm 0.2\%$) were exposed to different stress conditions. Fig. 5 gives an overview of iSEC chromatograms for HPV VLPs subjected to chemical, thermal, mechanical and freeze–thaw stress conditions. Chromatograms were normalized to the VLP monomer peak to highlight changes in aggregate levels.

Fig. 5a depicts the impact of ionic strength and buffer components on the VLP aggregate level. VLPs that were buffer-exchanged and stored for three days in a phosphate buffer without additional neutral salt revealed the highest level of aggregates ($9.6 \pm 0.2\%$), while the lowest aggregate level was observed for VLPs stored in 0.2 M MOPS with 0.5 M NaCl ($6.7 \pm 0.2\%$). In general, there was a clear trend of a decrease in aggregate levels with increasing salt concentrations and with MOPS buffers instead of phosphate buffers. Both buffer components are usually used during purification of HPV VLPs by cation-exchange (CEX) chromatography and mixed-mode (MM) chromatography [45]. Fig. 5b shows the effect of exposure to an elevated temperature (40 °C) on the formation of VLP aggregates. An increase in aggregate levels from $5.8 \pm 0.2\%$ to $10.4 \pm 0.3\%$ was observed after sample incubation for five hours at 40 °C. Aggregate levels steadily increased with increasing heat exposure time. Thermal stability studies are especially important to assess risks arising due to interrupted cold chains or inadequate storage conditions. The obtained results demonstrate that the investigated stabilized and formulated HPV VLPs are prone to form aggregates when exposed to 40 °C for more than 1 h. In contrast, Fig. 5c and 5d indicate that mechanical stress such as intense mixing for up to 24 h and numerous freeze-thaw cycles hardly change the dispersity of HPV VLPs in the used formulation buffer. Aggregate levels vary between $5.8 \pm 0.2\%$ and $6.7 \pm 0.2\%$. This confirms the findings of Shi et al. [13] identifying the non-ionic surfactant polysorbate 80 as stabilizer for HPV VLPs during freezing and reconstitution as well as mechanical stress conditions.

4. Conclusion and outlook

In this work, we report the development and application of a high-throughput analytical tool for the characterization of virus-like particles. Recently, the relevance of SE-HPLC methods for viral vaccines has been highlighted by Yang et al. [20]. Using a low-dispersion UHPLC system, we identified an SRT 1000 column as optimal SEC column for quantification of VLP aggregates at low buffer consumption and high flow rates. The implementation of an interlaced SE-UHPLC procedure allowed the characterization of VLPs within 3.1 min. To the best of our knowledge, this represents the fastest so far reported method for the quantification of VLP aggregates. The feasibility of the assay was proven for a variety of VLPs with total particle sizes ranging from 20 to 120 d nm. The VLP characterization by the iSEC method was supported and complemented by TEM and DLS measurements. In two case studies applying the assay, we demonstrated how aggregate levels are impacted by both downstream processing and storage of VLPs. Promising conditions for aggregate removal by precipitation with polyethylene glycol were determined applying high-throughput experimentation on a robotic liquid-handling station. The developed analytical method enables rapid assessment of suitable purification and formulation procedures for VLPs. In order to ensure both safety and immunogenicity of VLP vaccines, it will be important to specify acceptable and alarm limits for VLP aggregates, identify critical process parameters (ICH Q7 [46]), and define design spaces for production processes (ICH Q8 [47]). A potential well-suited process analytical technique for this purpose has been presented herein.

Acknowledgements

The authors gratefully acknowledge material supply by Diarect AG, Merck & Co, Sentinext Therapeutics, BioNTech Protein Therapeutics, Tosoh Bioscience and financial support from the German Federal Ministry of Education and Research (Grant agreement 0315640B). In addition, we would like to thank Mohammad Fotouhi from the KIT Laboratory for Electron Microscopy for acquisition of TEM micrographs, Thiemo Huuk for his support regarding UHPLC methods, Ozan Ötes for performing part of the experimental work, and Mike Kosinski (Merck & Co), René Djurup, Jane Cardosa (Sentinext Therapeutics), Fiona K. Hughes and Nani Wibowo (The University of Queensland) for their support regarding VLP handling and technology transfer. This research work is part of the project 'Optimization of an industrial process for the production of cell-culture-based seasonal and pandemic influenza vaccines'.

Conflict of interest: The authors declare no conflict of interest.

References

[1] Zeltins A. Construction and characterization of virus-like particles: a review. Mol Biotechnol 2013;53(1):92–107, http://dx.doi.org/10.1007/s12033-012-9598-4.

[2] Lua LHL, Connors NK, Sainsbury F, Chuan YP, Wibowo N, Middelberg APJ. Bioengineering virus-like particles as vaccines. Biotechnol Bioeng 2014;111(3):425–40, http://dx.doi.org/10.1002/bit.25159.

[3] Buonaguro L, Tagliamonte M, Visciano ML, Andersen H, Lewis M, Pal R, et al. Immunogenicity of HIV virus-like particles in rhesus macaques by intranasal administration. Clin Vaccine Immunol 2012;19(6):970–3, http://dx.doi.org/10.1128/CVI.00068-12.

[4] Low JGH, Lee LS, Ooi EE, Ethirajulu K, Yeo P, Matter A, et al. Safety and immunogenicity of a virus-like particle pandemic influenza A (H1N1) 2009 vaccine: results from a double-blinded, randomized Phase I clinical trial in healthy Asian volunteers. Vaccine 2014;32(39):5041–8, http://dx.doi.org/10.1016/j.vaccine.2014.07.011.

[5] Sun Y, Carrion R, Ye L, Wen Z, Ro Y-T, Brasky K, et al. Protection against lethal challenge by Ebola virus-like particles produced in insect cells. Virology 2009;383:12–21, http://dx.doi.org/10.1016/j.virol.2008.09.020.

[6] Vekemans J, Leach A, Cohen J. Development of the RTS,S/AS malaria candidate vaccine. Vaccine 2009;27(Suppl 6):G67–71, http://dx.doi.org/10.1016/j.vaccine.2009.10.013.

[7] Middelberg APJ, Rivera-Hernandez T, Wibowo N, Lua LHL, Fan Y, Magor G, et al. A microbial platform for rapid and low-cost virus-like particle and capsomere vaccines. Vaccine 2011;29(41):7154–62, http://dx.doi.org/10.1016/j.vaccine.2011.05.075.

[8] Klamp T, Schumacher J, Huber G, Kühne C, Meissner U, Selmi A, et al. Highly specific auto-antibodies against claudin-18 isoform 2 induced by a chimeric HBcAg virus-like particle vaccine kill tumor cells and inhibit the growth of lung metastases. Cancer Res 2011;71(2):516–27, http://dx.doi.org/10.1158/0008-5472.CAN-10-2292.

[9] Bachmann MF, Whitehead P. Active immunotherapy for chronic diseases. Vaccine 2013;31(14):1777–84, http://dx.doi.org/10.1016/j.vaccine.2013.02.001.

[10] Metz B, van den Dobbelsteen G, van Els C, van der Gun J, Levels L, van der Pol L, et al. Quality-control issues and approaches in vaccine development. Expert Rev Vaccines 2009;8:227–38, http://dx.doi.org/10.1586/14760584.8.2.227.

[11] Ladd Effio C, Hubbuch J. Next generation vaccines and vectors: Designing downstream processes for recombinant protein-based virus-like particles. Biotechnol J 2015;10:715–27, http://dx.doi.org/10.1002/biot.201400392.

[12] Carrondo MJT, Alves PM, Carinhas N, Glassey J, Hesse F, Merten OW, et al. How can measurement, monitoring, modeling and control advance cell culture in industrial biotechnology? Biotechnol J 2012;7:1522–9, http://dx.doi.org/10.1002/biot.201200226.

[13] Shi L, Sanyal G, Ni A, Luo Z, Doshna S, Wang B, et al. Stabilization of human papillomavirus virus-like particles by non-ionic surfactants. J Pharm Sci 2005;94(7):1538–51, http://dx.doi.org/10.1002/jps.20377.

[14] Zhao Q, Allen MJ, Wang Y, Wang B, Wang N, Shi L, et al. Disassembly and reassembly improves morphology and thermal stability of human papillomavirus type 16 virus-like particles. Nanomedicine 2012;8:1182–9, http://dx.doi.org/10.1016/j.nano.2012.01.007.

[15] Yu Z, Reid JC, Yang Y-P. Utilizing dynamic light scattering as a process analytical technology for protein folding and aggregation monitoring in vaccine manufacturing. J Pharm Sci 2013;102:4284–90, http://dx.doi.org/10.1002/jps.23746.

[16] Lang R, Winter G, Vogt L, Zurcher a, Dorigo B, Schimmele B. Rational design of a stable, freeze-dried virus-like particle-based vaccine formulation. Drug Dev Ind Pharm 2009;35:83–97, http://dx.doi.org/10.1080/03639040802192806.

[17] Citkowicz A, Petry H, Harkins RN, Ast O, Cashion L, Goldmann C, et al. Characterization of virus-like particle assembly for DNA delivery using asymmetrical flow field-flow fractionation and light scattering. Anal Biochem 2008;376:163–72, http://dx.doi.org/10.1016/j.ab.2008.02.011.

[18] Pease LF, Lipin DI, Tsai D-H, Zachariah MR, Lua LHL, Tarlov MJ, et al. Quantitative characterization of virus-like particles by asymmetrical flow field flow fractionation, electrospray differential mobility analysis, and transmission electron microscopy. Biotechnol Bioeng 2009;102:845–55, http://dx.doi.org/10.1002/bit.22085.

[19] Deschuyteneer M, Elouahabi A, Plainchamp D, Plisnier M, Soete D, Corazza Y, et al. Molecular and structural characterization of the L1 virus-like particles that are used as vaccine antigens in Cervarix™, the AS04-adjuvanted HPV-16 and -18 cervical cancer vaccine. Hum Vaccine 2010;6:407–19, http://dx.doi.org/10.4161/hv.6.5.11023.

[20] Yang Y, Li H, Li Z, Zhang Y, Zhang S, Chen Y, et al. Size-exclusion HPLC provides a simple, rapid, and versatile alternative method for quality control of vaccines by characterizing the assembly of antigens. Vaccine 2015;33:1143–50, http://dx.doi.org/10.1016/j.vaccine.2015.01.031.

[21] Fekete S, Beck A, Veuthey J-L, Guillarme D. Theory and practice of size exclusion chromatography for the analysis of protein aggregates. J Pharm Biomed Anal 2014;101:161–73, http://dx.doi.org/10.1016/j.jpba.2014.04.011.

[22] Tekewe A, Connors NK, Sainsbury F, Wibowo N, Lua LH, Middelberg AP. A rapid and simple screening method to identify conditions for enhanced stability of modular vaccine candidates. Biochem Eng J 2015;100:50–8, http://dx.doi.org/10.1016/j.bej.2015.04.004.

[23] Schmidt U, Rudolph R, Böhm G. Mechanism of assembly of recombinant murine polyomavirus-like particles. J Virol 2000;74:1658–62.

[24] Li Y, Bi J, Zhou W, Huang Y, Sun L, Zeng A-P, et al. Characterization of the large size aggregation of Hepatitis B virus surface antigen (HBsAg) formed in ultrafiltration process. Process Biochem 2007;42(3):315–9, http://dx.doi.org/10.1016/j.procbio.2006.08.016.

[25] Huang Y, Bi J, Zhang Y, Zhou W, Li Y, Zhao L, Su Z. A highly efficient integrated chromatographic procedure for the purification of recombinant hepatitis B surface antigen from Hansenula polymorpha. Protein Exp Purif 2007;56:301–10, http://dx.doi.org/10.1016/j.pep.2007.08.009.

[26] Yu M, Zhang S, Zhang Y, Yang Y, Ma G, Su Z. Microcalorimetric study of adsorption and disassembling of virus-like particles on anion exchange chromatography media. J Chromatogr A 2015;1388:195–206, http://dx.doi.org/10.1016/j.chroma.2015.02.048.

[27] Farnan D, Moreno GT, Stults J, Becker A, Tremintin G, van Gils M. Interlaced size exclusion liquid chromatography of monoclonal antibodies. J Chromatogr A 2009;1216:8904–9, http://dx.doi.org/10.1016/j.chroma.2009.10.045.

[28] Diederich P, Hansen SK, Oelmeier SA, Stolzenberger B, Hubbuch J. A sub-two minutes method for monoclonal antibody-aggregate quantification using parallel interlaced size exclusion high performance liquid chromatography. J Chromatogr A 2011;1218:9010–8, http://dx.doi.org/10.1016/j.chroma.2011.09.086.

[29] Kim K, Park S, Ko K. Current status of human papillomavirus vaccines. Clin Exp Vaccine Res 2014;3:168–75, http://dx.doi.org/10.7774/cevr.2014.3.2.168.

[30] Lim P-Y, Hickey AC, Jamiluddin MF, Hamid S, Kramer J, Santos R, et al. Immunogenicity and performance of an enterovirus 71 virus-like-particle vaccine in nonhuman primates. Vaccine 2015:1–8, http://dx.doi.org/10.1016/j.vaccine.2015.05.108.

[31] Chandramouli S, Medina-Selby A, Coit D, Schaefer M, Spencer T, Brito LA, et al. Generation of a parvovirus B19 vaccine candidate. Vaccine 2013;31(37):3872–8, http://dx.doi.org/10.1016/j.vaccine.2013.06.062.

[32] Ladd Effio C, Wenger L, Ötes O, Oelmeier Sa, Hubbuch J. Downstream processing of virus-like particles: single-stage and multi-stage aqueous two-phase extraction. J Chromatogr A 2015;1383:35–46, http://dx.doi.org/10.1016/j.chroma.2015.01.007.

[33] Effio CL, Hahn T, Seiler J, Oelmeier SA, Asen I, Silberer C, Villain L, Hubbuch J. Modeling and simulation of anion-exchange membrane chromatography for purification of Sf9 insect cell-derived virus-like particles. J. Chromatogr. A 2015;1429:142–54, http://dx.doi.org/10.1016/j.chroma.2015.12.006.

[34] Wiendahl M, Völker C, Husemann I, Krarup J, Staby A, Scholl S, et al. A novel method to evaluate protein solubility using a high throughput screening approach. Chem Eng Sci 2009;64:3778–88, http://dx.doi.org/10.1016/j.ces.2009.05.029.

[35] Oelmeier S, Ladd-Effio C, Hubbuch J. Alternative separation steps for monoclonal antibody purification: Combination of centrifugal partitioning chromatography and precipitation. J Chromatogr A 2013;1319:118–26.

[36] ICH Guideline Q2. Validation of analytical procedures: text and methodology; 1994.

[37] Erickson HP. Size and shape of protein molecules at the nanometer level determined by sedimentation, gel filtration, and electron microscopy. Biol Proc Online 2009;11(1):32–51, http://dx.doi.org/10.1007/s12575-009-9008-x.

[38] Yang R, Tang Y, Zhang B, Lu X, Liu A, Zhang YT. High resolution separation of recombinant monoclonal antibodies by size-exclusion ultra-high performance liquid chromatography (SE-UHPLC). J Pharm Biomed Anal 2015;109:52–61.

[39] Zhao Q, Guo HH, Wang Y, Washabaugh MW, Sitrin RD. Visualization of discrete L1 oligomers in human papillomavirus 16 virus-like particles by gel electrophoresis with Coomassie staining. J Virol Methods 2005;127:133–40, http://dx.doi.org/10.1016/j.jviromet.2005.03.015.

[40] Mohr J, Chuan YP, Wu Y, Lua LHL, Middelberg APJ. Virus-like particle formulation optimization by miniaturized high-throughput screening. Methods 2013;60(3):248–56, http://dx.doi.org/10.1016/j.ymeth.2013.04.019.

[41] Liu C-C, Guo M-S, Lin FH-Y, Hsiao K-N, Chang KH-W, Chou A-H, et al. Purification and characterization of enterovirus 71 viral particles produced from vero cells grown in a serum-free microcarrier bioreactor system. PLoS One 2011;6, http://dx.doi.org/10.1371/journal.pone.0020005.

[42] Bernstein DI, El Sahly HM, Keitel Wa, Wolff M, Simone G, Segawa C, et al. Safety and immunogenicity of a candidate parvovirus B19 vaccine. Vaccine 2011;29(43):7357–63, http://dx.doi.org/10.1016/j.vaccine.2011.07.080.

[43] Jain NK, Sahni N, Kumru OS, Joshi SB, Volkin DB, Russell Middaugh C. Formulation and stabilization of recombinant protein based virus-like particle vaccines. Adv Drug Deliv Rev 2016, http://dx.doi.org/10.1016/j.addr.2014.10.023.

[44] Giese G, Myrold A, Gorrell J, Persson J. Purification of antibodies by precipitating impurities using Polyethylene Glycol to enable a two chromatography step process. J Chromatogr B Anal Technol Biomed Life Sci 2013;938:14–21, http://dx.doi.org/10.1016/j.jchromb.2013.08.029.

[45] Cook III JC. Process for purifying human papillomavirus virus-like particles, US Patent 6,602,697 (August 5, 2003).

[46] ICH Guideline Q7. Good manufacturing practice for active pharmaceutical ingredients; 2000.

[47] ICH Guideline Q8. Pharmaceutical development; 2006.

[48] Karpenko LI, Ivanisenko VA, Pika IA, Chikaev NA, Eroshkin AM, Veremeiko TA, et al. Insertion of foreign epitopes in HBcAg: how to make the chimeric. Amino Acids 2000;18:329–37.

[49] Lin S-Y, Chiu H-Y, Chiang B-L, Hu Y-C. Development of EV71 virus-like particle purification processes. Vaccine 2015:1–8, http://dx.doi.org/10.1016/j.vaccine.2015.04.077.

[50] Kaufmann B, Simpson AA, Rossmann MG. The structure of human parvovirus B19. Proc Natl Acad Sci U S A 2004;101(32):11628–33, http://dx.doi.org/10.1073/pnas.0402992101.